Investigation of Operational Parameters on the Photocatalytic Activity of a New Type of Poly(methyl methacrylate)/Ionic Liquid-TiO_2 Nanocomposite

Mirhoseini, Farid
Department of Chemistry, Faculty of Science, Arak University, 38156-8-8349, Arak, I.R. IRAN

Salabat, Alireza*+
Institue of Nanosciences & Nanotechnolgy, Arak University, 38156-8-8349, Arak, I.R. IRAN

ABSTRACT: *This research work intended to study some important operational parameters on the photocatalytic activity of a new type of poly(methyl methacrylate) (PMMA)/IL-TiO_2 nanocomposite, prepared by microemulsion method. For the first step, it is confirmed that the prepared nanocomposite has a significant effect on photodecomposition of the Trypan Blue (TB), as an anionic hydrophilic azo dye, and good antibacterial activity against Bacillus spp., as Gram positive bacteria, under visible light. After that, the operational parameters such as TiO_2 content in photocatalyst, the thickness of the nanocomposite film, visible light intensity, and pH of the solution have been studied. In order to have a precise study on the photocatalytic performance of the prepared nanocomposite, the hydroxyl radical dosage in photocatalytic experiments and oxidative stress in the antibacterial experiment have been measured. This strategy was performed to show the extreme effect of TiO_2 dosage on the photocatalytic activity of the nanocomposite.*

KEYWORDS: *Poly(methyl methacrylate), Ionic liquid, TiO_2 nanoparticles, Photodecomposition, Nanocomposite.*

INTRODUCTION

For the past two decades, polymer/TiO_2 nanocomposites as nanotechnological products have vast potential in the commercialization and also in business, especially in water treatment [1,2], self-cleaning [3] and antibacterial surfaces [4]. Titanium dioxide (TiO_2) due to a broad range of excellent properties, such as safe to use and no secondary pollution to environment has attracted much attention for the past few decades as the most promising photocatalyst [5]. Photocatalysis has also been used extensively to kill microbial species and decomposition of pollutants in water and air [4]. Some of the reasons for the interest combining photocatalysis and polymers material is minimizing photocatalyst loss, availability of longer contact time, ease of post-treatment

* *To whom correspondence should be addressed.*
+ *E-mail: a-salabat@araku.ac.ir*
1021-9986/2019/4/101-114 14/$/6.04

recovery and very advantageous for human health [6,7]. PMMA as a hydrophobic polymer with low surface energy was chosen as a matrix to immobilize of TiO_2 nanoparticles, because of UV transparency and easy mouldable [8]. TiO_2 can be applied as an effective photocatalyst just when exposed to UltraViolet (UV) irradiation [9].

To overcome the above mentioned drawback, continuous efforts are being investigated to look for visible light as an alternative source of illumination for TiO_2 photocatalyst [1]. Low density polyethylene (LDPE)–TiO_2 films produced by *Ratova et al*. [4] with an extrusion method and its photocatalytic antibacterial activity was tested via the destruction of *Escherichia coli* with 30 *wt*.% of TiO_2. They also investigated the photodecomposition of methylene blue dye under UV illumination by LDPE–TiO_2 films. In order to make applicable TiO_2 photocatalyst in visible light, several approaches such as sensitization by noble metals have been reported [10-13]. Comparing the previous works in this study, the PMMA/IL-TiO_2 nanocomposite seems to be very promising photocatalyst at very low loading of TiO_2. Additionally, the scope for preparation of visible light sensitization of PMMA/TiO_2 nanocomposite without doping agents has been highlighted. By using the ionic liquid based microemulsion system, a polymer-TiO_2 nanocomposite can be deduced which not only is visible light active photocatalyst without any additive but also improves the recombination of photogenerated holes and electron as the major limitation of polymer-TiO_2 mediated photocatalysis.

Large amounts of colored wastewater that are difficult to decompose are generated in many industries and have a serious environmental risk. Wastewater containing dyes are discharged into natural hydric bodies and cause severe contaminations to the drinking water and irrigation systems in some areas with undesirable consequences to the environment and to human health [14]. Trypan blue is an anionic acid dye that as carcinogens can kill trypanosomes, the parasites that cause sleeping sickness. Exposure to the material for prolonged periods may cause physical defects in the developing embryo (teratogenesis) and also caused death, apparently in central nervous system depression by the State of California environmental protection agency (2009) [15].

As per our pervious literature survey, the PMMA/TiO_2 nanocomposite as heterogeneously photocatalysis method is superior route than the conventional dye removal methods [16.17]. In progressing our research works in waste water treatment [2], we considered in this study the photodegradation of Trypan Blue (TB) as a diazo dye compound that is characterized by the presence of the azo group (-N=N-) as illustrated in scheme 1.

As far as we know, *Elfeky et al*. [18] investigated photodecomposition of TB dye under sunlight by Au-TiO_2 (0.08g)/PMMA thin film nanocomposite that was prepared via TiO_2 suspended in PMMA dissolved in tetrahydrofuran (THF). They observed that degradation efficiency was 90% by Au-TiO_2 (0.08g)/PMMA thin film after 1.75 h at pH = 2 and 87% in 2.5 h by TiO_2 (0.08g)-PMMA thin film under similar conditions. Hence, in continuation of our research works on microemulsion systems as soft template for nanomaterials synthesis [2,19,24] the chief object of the present examination is to focus on some environmental applications of PMMA/TiO_2 nanocomposite, prepared by ionic liquid based microemulsion.

In our previous report, PMMA/IL-TiO_2 nanocomposite as a highly efficient visible light photocatalyst was synthesized and characterized [2]. In the current work, some important operational parameters on the photocatalytic activity of the prepared PMMA/TiO_2/IL nanocomposite have been investigated. The effects of TiO_2 dosage, pH, the light intensity of lamp, and thickness of the prepared film on the rate constant of TB photodecomposition were determined. As a second application, the antibacterial effect of the nanocomposite was tested on the destruction of the clinical strain of *Bacillus* sp (ATCC 49342) bacteria (Gram-positive) in the harvest of visible light based on oxidative stress and cell permeability. Our strategy in this research, which is different from the previous works, is the measurement of hydroxyl radical during the photocatalysis process for assessment of the effect of TiO_2 dosage on photocatalytic activity.

EXPERIMENTAL SECTION

Materials and method

Hydrophilic ionic liquid, ([bmim][BF_4]), the nonionic surfactant of Triton X-100 and the 2́,7́-Dichloro

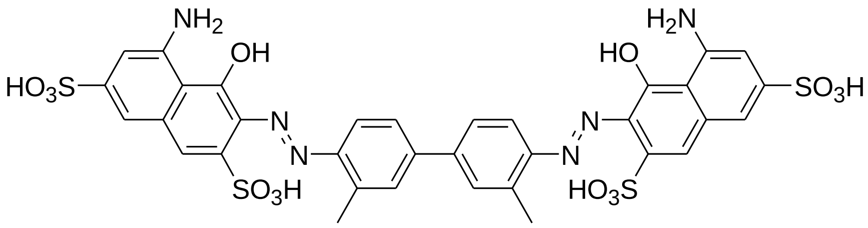

Scheme 1: TB dye chemical structure.

fluorescein diacetate (DCFH-DA), were purchased from Sigma-Aldrich. The titanium dioxide TiO_2 nanoparticles used in this study was Degussa P25 (ca. 80% anatase, 20% rutile, with a BET surface area of 50 m^2/g and particle size of less than 15 nm). Methyl methacrylate (MMA) monomer (AR grade), benzoyl peroxide (BPO), 1-butanol, HNO_3, NaOH and salicylic acid (as a probe molecule) reagents (analytical grade) were received from Merck. Trypan blue as a pollutant model used as received. All aqueous solutions were prepared with deionized water (0.055 µS/cm) which was produced in our lab with PKA (Smart two pure) instruments.

Preparation of the modified PMMA/IL-TiO_2 nanocomposite film

In order to synthesis modified PMMA/IL-TiO_2 nanocomposite a microemulsion system consisting of hydrophilic ionic liquid [bmim][BF_4] as polar phase, MMA as apolar phase, TX-100 and 1-buthnol as co-surfactant was prepared at different loading of TiO_2 as explained in our previous work [2]. Benzoyl peroxide (BPO) as an initiator was added to the above stabilized TiO_2 colloidal systems and the vial was put into a 60°C oil-bath for 5 h to start polymerization process. The transparent and viscose gel was obtained. Then the prepared gel was substituted on the glass plate and was converted to a film using an automatic film applicator (ELCOMETER). Fig. 1 demonstrates a schematic illustration of the automatic film applicator set-up.

For labeling purposes, the resultant transparent nanocomposite films of PMMA/IL-TiO_2 were marked like S0, S1, S2 and S3 refer to the amounts of TiO_2 nanoparticles corresponding to 0.000, 0.008, 0.010 and 0.012 wt.%. No apparent visible phase separation was observed during the polymerization process for all samples. Pure PMMA was also prepared under the same condition and identically formulated microemulsion without TiO_2 loading which was labelled as S0. All of the produced transparent films had the uniform thickness with an average central thickness of 100 µm, as measured using a micrometer. Techniques such as UV-Vis Diffuse Reflectance Spectra (DRS), TEM, FT-IR and TGA were used to characterize the resulting modified nanocomposite and reported in our previous paper. The obtained UV-Vis diffuse reflectance spectrums for the sensitized PMMA/TiO_2 nanocomposites by ionic liquid and original TiO_2 confirmed that the absorbance shifted greatly toward a red light and its band gap was obtained equal to 2.55 *eV* (Fig. 2).

TEM micrograph for the PMMA/IL-TiO_2 nanocomposite confirmed a core-shell structure for the nanocomposite with an average particle size of about 11 nm. This structure has a ring of titania as a shell with darker regions around the soft IL domains as a core corresponded to brighter regions, which wrapped in a hard "continuous" polymeric matrix. TEM image for core-shell structure of the PMMA/IL-TiO_2 nanocomposite has been shown in Fig. 3.

Photoreactor and Photodecomposition of TB

All the nanocomposites were initially assessed for the photodegradation of TB at normal laboratory environmental conditions. The photodecomposition experiment was carried out in a glass beaker as the reaction vessel. The photocatalyst was irradiated with a fluorescence lamp as the light source which was attached vertically at the top. Fluorescence lamps manufactured by Pars Shahab Company (Iran) and their emission spectrums were presented in Fig. ES1. The distance between the light and the reactor was fixed at 10 cm. The assembled system was placed inside a wooden box coloured black so that no stray light can inter the reactor.

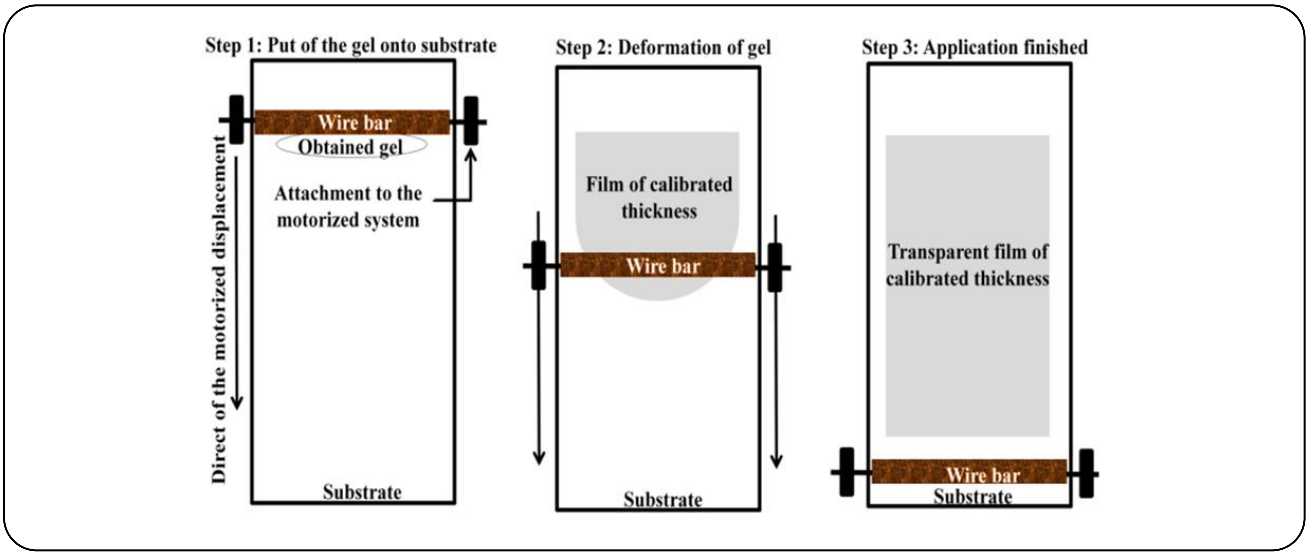

Fig. 1: Schematic demonstration of automatic film applicator set-up.

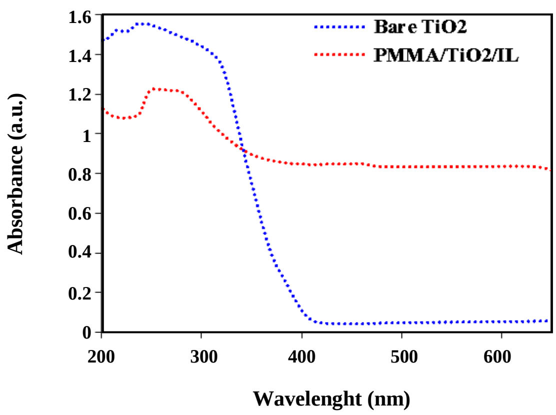

Fig. 2: UV–Vis diffuses reflectance spectra of the original TiO_2 and prepared nanocomposite.

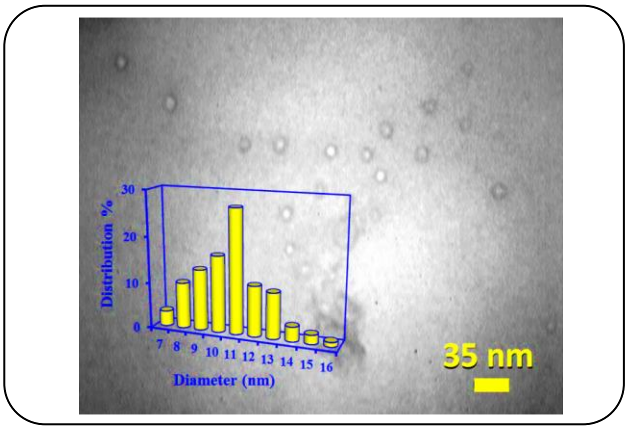

Fig. 3: TEM image of PMMA/TiO_2/IL nanocomposite.

In a typical experiment, the desired weight of the catalyst was heterogeneously suspended in a 5 ml, 10^{-5} M of TB dye solution as a representative example of a photocatalytic reaction. The reaction was carried out isothermally at 25 °C, and samples of the reaction mixture analyzed at different time intervals for a total reaction time of 6 h. During the photodecomposition process, the UV−visible spectra of the reaction mixture were recorded at intervals of 30 min. Before analyzing with a double beam UV-vis spectrophotometer (Perkin Elmer lambda 15), the nanocomposite film was removed from all solutions to stop the reaction. A control sample as blank, which referred to a solution of TB without photocatalyst was employed.

Measurement of Hydroxyl Radical

The hydroxyl radical is a powerful oxidizing species that is generated upon proper photon irradiation to nanocomposite film. The hydroxyl radical has potential oxidation of approximately 2.8 volts (versus NHE), which may lead to complete degradation or mineralization of pollutants and the photocatalytic activity is directly related to the amount of $^{\bullet}OH$ radicals. The effect of TiO_2 content in the nanocomposites on the amount of produced hydroxyl radicals was performed using salicylic acid as a probe molecule [25,26]. In this method, the 2,3-dihydroxybenzoic acid formed due to reaction of the salicylic acid with the hydroxyl radicals after reacting 60 min. The amounts of hydroxyl radicals were measured by UV-Vis absorption spectrophotometric method at wavelength of 510 nm. A blank experiment was run before adding the nanocomposite to the salicylic acid solution. The result confirmed that there was no photolysis reaction in salicylic acid under visible light illumination without nanocomposite. Fig. ES2 shows the absorbance of the produced 2,3-dihydroxybenzoic acid against the amount of TiO_2 contents in the nanocomposite film under visible light irradiation. From this figure it can be concluded that the amount of produced hydroxyl radical is maximum for S2 nanocomposite sample.

Antibacterial activity test (Kirby-Bauer method and membrane permeability assessments)

The photocatalytic-based antibacterial properties of the produced nanocomposite films (S1-S3) and pure PMMA film (S0) as control sample were analyzed by the agar well diffusion method [27-29], against a clinical isolate *Bacillus* sp. (ATCC 49342) bacterium (from Gram-positive) as representative bacterial strain same to our previous report in a thermostatic light incubator under visible light irradiation [30]. This procedure was repeated three times. The calibrated thickness of the nanocomposite film for this study was 90 μm.

In order to confirm the Kirby-Bauer method for the determination of the antibacterial activity of nanocomposite samples another method based on membrane permeability assessments performed. A membrane permeability evaluation based on extracellular lactate dehydrogenase (LDH) enzyme which acts as an indicator of membrane permeability was performed The level of LDH released was examined after interact of the bacterial suspension of individual isolate *Bacillus* with the entire nanocomposite samples and compared with pure PMMA as control. To do this study the cells were centrifuged for 10 min and the supernatant was measured based on the standard protocol [31, 32].

The fluorescent probe DCFH-DA method was used to quantify a number of Reactive Oxygen Species (ROS) [32,33]. The proposed mechanism for the quantification of ROS is based on the DCFH-DA oxidation to 2'-7'-dichlorofluorescein (DCF). The generation of ROS was investigated in PMMA blank and S1, S2 and S3 nanocomposites interacted with individual bacterial cells for 24 h. In this procedure the prepared bacterial cell suspension (5 mL) with DCFH-DA (100 μM) and all of the samples were incubated for 30 min under visible light illumination. Fluorescence intensity was checked by a fluorescence spectrophotometer (SHIMADZU RF-6000), with an excitation wavelength of 485 nm and an emission wavelength of 530 nm.

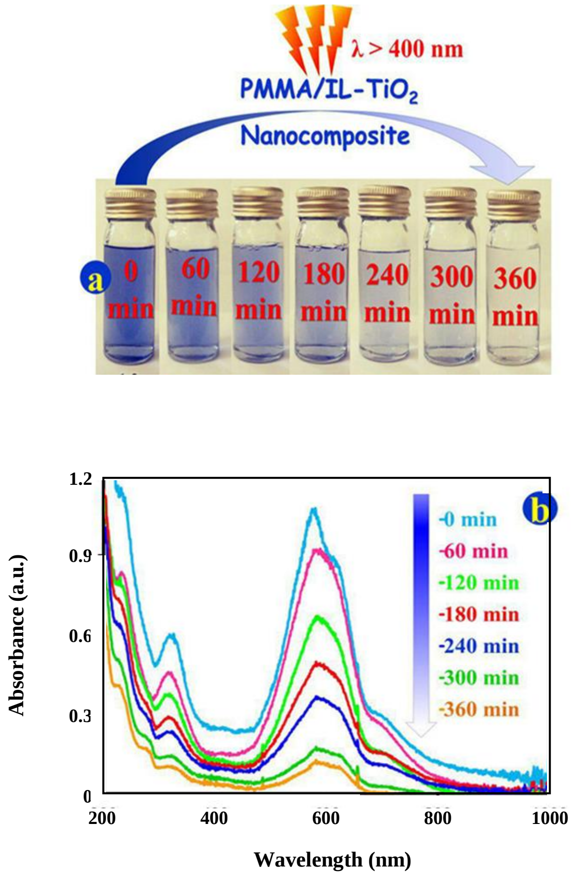

Fig. 3: Spectral patterns of TB dye solution during the photodecomposition process in the presence of S2 nanocomposite sample, under visible-light irradiation for 6 h.

RESULTS AND DISCUSSION

Effect of TiO_2 contents in the nanocomposites on TB photodecomposition

In order to study the kinetic of the photodegradation process by UV-visible method, a time-dependent spectrum for photodecomposition of TB dye solution containing nanocomposite (for S2 sample) was obtained and shown in Fig. 4.

As can be seen, the absorption band of the TB dye at ca. 585 nm decreased with increasing time [18]. The photocatalytic activity of the prepared nanocomposites was tested in photodecomposition of TB dye in an aqueous solution. Fig. 5 shows the photodecomposition

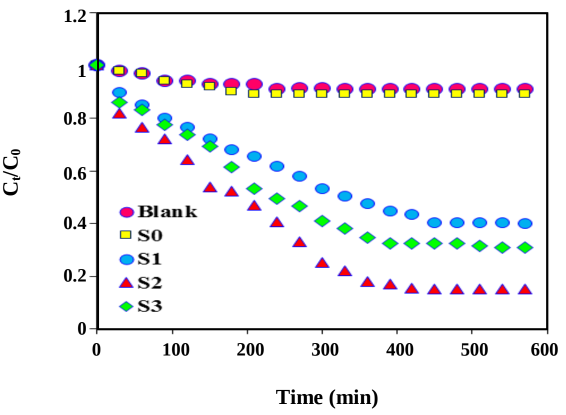

Fig. 5: Effect of TiO_2 nanoparticles concentration of PMMA/TiO_2 photocatalyst on photodecomposition of TB dye under visible light irradiation. The experiment was carried out under the following conditions: 10^{-5} M of TB dye solution, 0.009 g photocatalyst, 60 µm thickness of photocatalyst film.

process without photocatalyst (blank), pure PMMA and all of the nanocomposite samples. The UV−Visible spectrophotometric analysis substantiated that the modified PMMA/IL-TiO_2 served as a photocatalyst for the photodegradation reaction. A blank experiment shows that, without the addition of the photocatalyst, the photodegradation of TB is slow and the photodegradation efficiency is less than 9% after 6 h of visible light illumination.

As can be seen from Fig. 5, the concentration of TB dye decreased as a function of irradiation time. The maximum photodegradation efficiency was 82 %, belonging to Sample S2, after 6 h irradiating. As we expressed in our previous work, which was the photocatalytic degradation of MB as a cationic dye, it is clearly found that the ionic liquid sensitized TiO_2 immobilized in PMMA could be an effective catalyst for the water treatment process [2].

As can be seen from the results of this research the behavior of the nanocomposite against photocatalytic degradation of TB as an anionic dye is the same as cationic dye. As reported in the previous research works, the photodegradation of TB over the prepared nanocomposite produces several organic intermediates, particularly organic acids such as maleic acid, acetic and formic acid. On the other hand by the following mechanism inorganic final products can be expected [33-37]:

TB dye + $^{\bullet}OH$, $O_2^{\bullet -}$ or $HO_2^{\bullet}$ → SO_4^{2-}, NO_3^-, NH_4^+, CO_2, and H_2O

The photodecomposition rate constant was calculated by plotting *ln(C_0/C_t)* versus times based on the first order reaction according to the following equation.

$$\ln\frac{C_0}{C_t} = kt \tag{1}$$

Where *k* is the rate constant of the photodecomposition (min^{-1}), C_t and C_0 are the time-dependent concentration and initial concentration, respectively. The result of *ln*(C_0/C_t) versus the reaction time exhibits a good linear correlation. The calculated rate constants of photodegradation and the linear regression values are reported in Table 1. The rate constant toward the S2 sample of the photocatalyst was calculated as 40 × 10^{-4} min^{-1}, which was the maximum value. As shown in the results of Table 1, the rate constant was increased with the increasing dosage of TiO_2 and approaching a limiting value at higher loading of nanoparticles. This behaviour may be due to aggregation of nanoparticles in a polymer matrix which causing a decrease in the number of surface active sites. The rate constant trend against TiO_2 content of nanocomposites is compatible with the amount of produced hydroxyl radicals which explained in the previous section. It can be concluded that the amount of hydroxyl radicals increases as the TiO_2 content increases up to 0.010 wt.% (S2) and then decreases. Decreasing of the amount of generated hydroxyl radicals after S2 sample nay be related to the high recombination rate of photoinduced carriers for S3 sample (0.012 w% of TiO_2).

Effect of pH on the photodecomposition of TB dye

The pH value of the reaction medium during photodecomposition reactions plays a very significant role in the process design and control photocatalysts [2,18,38]. As the nature of the dye changed from cationic dye in our previous work to anionic dye in this research, it is necessary to investigate pH effect on the photodecomposition activity of the nanocomposites. The effect of pH on the photodecomposition of TB dye was evaluated by keeping all other conditions constant and varying the initial pH of the solution between 5 to11 and S2 sample of PMMA/IL-TiO_2 was used in this study. It is interesting that the higher efficiency was observed at pH value of 7 which is different to the optimum pH value of 8 for MB dye (Fig. 6).

Table 1: The calculated first-order rate constants of TB photodecomposition and the linear regression values.

Sample	$k \times 10^{-4}$(min^{-1})	R^2
Blank	5	0.9916
S0	5.5	0.9905
S1	23	0.9998
S2	40	0.9921
S3	26	0.9945

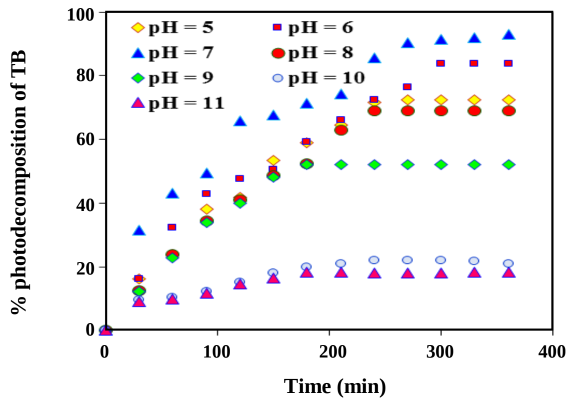

Fig. 6: Effect of solution pH on the TB photodecomposition over S2 nanocomposite sample under visible light irradiation. The experiment was carried out under the following conditions: 10^{-5} M of TB dye solution, 0.009 g photocatalyst, 60 µm thickness of photocatalyst film.

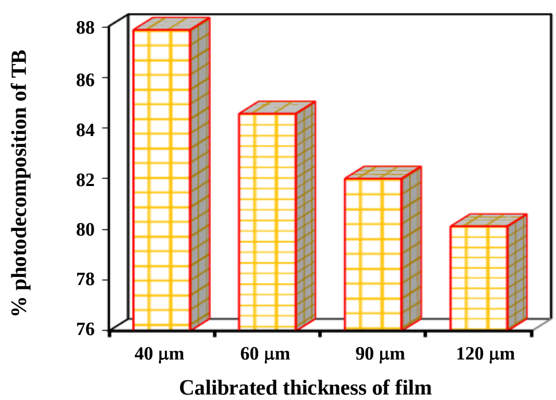

Fig. 7: Effect of calibrated thickness of photocatalyst film (S2) on the TB photodecomposition under visible light irradiation after 6 h. The experiment was carried out under the following conditions: 10^{-5} M of TB dye solution, 0.009 g photocatalyst.

It is clear that the change in the solution pH has a critical effect on the TB photodecomposition, which directly affects the surface charge properties of the photocatalyst and the adsorption of pollutants. As can be seen any further decrease or increase of pH less than 7 or more than 8, significantly decreases photocatalytic degradation efficiency. Therefore, it can be suggested an optimum value of 7 for pH in the photodecomposition process of TB dye with S2 Sample nanocomposite. We believe that the negative charge on the surface of this type of photocatalyst (PMMA/TiO_2/IL) is concentrated at pH = 7, favors adsorption of TB dye, and hence more photocatalytic activity will occur. This conclusion approves the effect of pH point of zero charge (pHPZC) of the photocatalyst which is about 6.5 on the catalytic activity. On the other words when pH is greater than pHPZC the photocatalyst is more effective. *Elfeky et al.* [18] investigated the TB photostability in neutral, acidic and basic media by TiO_2/PMMA thin film doped with Au. They observed that the maximum efficiency of photodecomposition of TB dye occurred at pH = 2. The obtained interesting result at pH = 7 may be related to the nature of the synthesized nanocomposite in IL-based microemulsion system. This behavior could be due to the effect of the electrostatic attraction between the positively charged nanocomposite surfaces and negatively charged sulfonic groups of dissociated TB [39, 40].

Effect of nanocomposite film thickness on the photodecomposition of TB dye

Fig. 7 shows that in the present of S2 Sample of PMMA/IL-TiO_2 nanocomposite film with a variety of thickness, the solution of TB dye had a light different in photodecomposition processes after 6 h of visible light irradiation. So, we may rule out the effect of calibrated thickness of nanocomposite film on the photodegradation of TB dye. As can be seen in Fig. 7, by decreasing nanocomposite film thickness the photodecomposition

Table. 2: Effect of power and intensity of lamp on the pseudo first-order rate constants of TB photodegradation, for S2 photocatalyst sample

Lamp power (W)	Total radiation (mW/cm^2)	$k \times 10^{-3}$(min^{-1})	R^2
60	0.141	4.0	0.9995
36	0.069	2.1	0.9967
18	0.035	1.8	0.9977

efficiency was increased. In our technique, the minimum thickness of the prepared film was 40 µm, which related to the maximum efficiency of 87.8 %. It may be due to that the film with smaller thickness is more capable of adsorption of visible light illumination. This phenomenon led to the increase in the generation of photoinduced holes and electrons and consequently the high formation of hydroxyl radicals and super oxide anion radical during the photocatalysis mechanism without recombination of charge carriers [2].

The effect of light intensity

The effect of light intensity as a series of photocatalytic experiments was studied under a variety of lamps to investigate of the TB photodecomposition rate by S2 Sample. A summary of the first order rate constants and linear regression values of kinetic data was reported in Table 2. As can be seen from Table 2, the rate constant value under 60 W irradiating was much higher than the other cases for TB photodecomposition. This result is in good agreement with the excellent generation of electron and holes pairs during the photocatalytic mechanism at the high intensity and consequently an increase in the photocatalytic efficiency. It was verified that the prepared PMMA/IL-TiO_2 nanocomposite as a visible light responsive photocatalyst capable to absorb visible light with different intensity and with increasing light intensity the photoactivity was enhanced [41].

Recycling and photocatalyst stability of the nanocomposite

The recycling and photocatalyst stability of the nanocomposite was investigated for photodegradation of TB dye after 6 runs at the same condition. As can be seen from Fig. ES3 the photocatalytic activity of the nanocomposite (Sample S2) does not show remarkable changes. This excellent result for fabricated nanocomposite film could be considered as an advantage parameter for its industrial application.

Antibacterial activity results

Antibacterial activity of the pure PMMA as a control sample and PMMA/IL-TiO_2 nanocomposites with various weight percentages of TiO_2 was evaluated under visible light irradiation toward *Bacillus* by the inhibition zone determination and the results were expressed as mm in Fig. 8. As can be seen, the PMMA/IL-TiO_2 nanocomposite with the maximum inhibition zone exhibits remarkable antibacterial activity against *Bacillus* upon exposure to visible light compared to the pure PMMA. As a consequence, with increasing TiO_2 loading in the nanocomposite film the photocatalyst-based antibacterial activity first increased and then decreased with further increasing of TiO_2 dosage more than 0.01%. The zones of inhibition with pure PMMA (as control), S1, S2 and S3 samples were obtained as 0, 6 ± 0.21, 19 ± 0.15 and 13 ± 0.46, respectively. The main killing mechanism for the antimicrobial effect of TiO_2 photocatalysis is attributed to the hydroxyl radicals and Reactive Oxygen Species (ROS) as part of the photocatalytic mechanism that was first proposed by *Matsunaga et al.* [42] and has been well reviewed consequently by others [43-46] and may be explained as follows. Degradation of the cell wall and cytoplasmic membrane by hydroxyl radicals and hydrogen peroxide due to their penetration ability into the bacteria cell envelope is a common mechanism. It should be noted that superoxide anion radicals ($^{\bullet}O_2^-$) do not exhibit such ability and act just on the cell wall. Finally, cell lysis followed by the complete mineralization of the organism [30, 47-49]. As other observations for antibacterial activity of the nanocomposite, it is interesting that in contrast to a conductive polymer, same as polypyrrole, no zone of inhibition can be detected for PMMA (Fig. 8). The electrostatic adsorption between conductive polymer and bacteria, higher molecular weight, surface hydrophilicity and direct contact between polymer and bacteria cell as key factors lead to the existence of antibacterial activity of

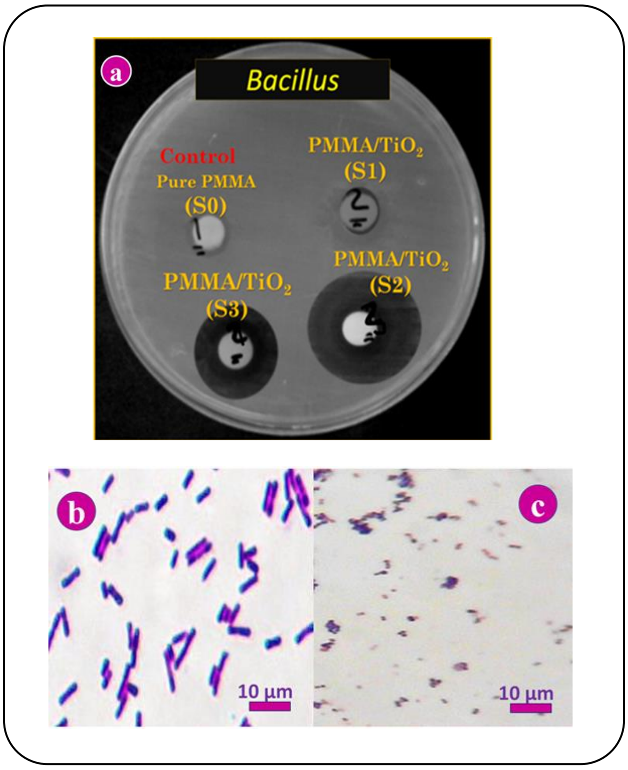

Fig. 8: (a) Antibacterial activity of clinical strain of Bacillus, with (1) Pure PMMA, (2) S1, (3) S2 and (4) S3, by Kirby-Bauer method, micrograph of (b) untreated and (c) treated Bacillus after 6 h against S2 sample under visible light irradiation.

pure conductive polymer [50, 51] and the direct comparison of results is rarely possible. So the hydrophobic nature of the PMMA as one of the main reasons leads to low bacterial adhesion and subsequently very low antibacterial activity [4].

The effect of the prepared nanocomposite (S2 Sample) on the morphology of *Bacillus* was examined by an Olympus optical microscope to confirm antibacterial activity during the photocatalytic treatment based on our previous report [52-54]. As seen in Fig. 8(a), untreated *Bacillus* cells exist as colonies of rod-shaped bacteria in native culture. Fig. 8(b) reveals the morphological changes of this rod-shaped structure after 6h treatment against the visible light irradiated on the S2 nanocomposite sample. This result confirms that the nanocomposite sample which was irradiated causes the structural changes in the cell membrane.

In our previous research work, we reported the antibacterial activity of prepared nanocomposite against *Escherichia coli*, *Klebsiella* and *Staphylococcus aureus* bacteria, that the nanocomposite film shown efficient photocatalytic activity at a very low dosage of TiO_2 [27]. However, oxidative stress was not considered precisely. In this study antibacterial activity of prepared nanocomposites was investigated on *Bacillus*. Oxidative stress and cell permeability were also investigated in detail. As can be seen from Fig. 9 the fluorescence intensity, which is related to the oxidative stress, is maximum for S2 sample. This result indicates that S2 sample has more antibacterial activity than other samples. It is well known that the antibacterial ability of a sample is because disrupting the cell membrane integrity through the generation of intracellular and extracellular reactive oxygen species [32,33]. To investigate this mechanism for the antibacterial activity of the nanocomposite samples the cell permeability method was also tested. The releases of an extracellular enzyme, lactate dehydrogenase (LDH) level were analyzed based on the prepared nanocomposite films interacted with the *Bacillus.* As can be seen from Fig. 10 the LDH release was observed to be much higher for S2 sample, confirming the fact that reactive oxygen species levels were comparatively higher than other nanocomposite samples as well as a control sample.

CONCLUSIONS

In this work, we confirmed that the PMMA/IL-TiO_2 nanocomposite film sensitized by the ionic liquid in microemulsion technique displays noticeable photocatalytic activity for cationic and anionic dyes as well as antibacterial activity. The best performance parameters of this special catalyst in the photodecomposition of an anionic dye and bacteriological study were obtained. It is also verified that using ionic liquid based microemulsion systems for the preparation of PMMA/IL-TiO_2 causes the high photocatalytic activity under visible light, as was mentioned in our previous work, and its applicability can be developed. This could be associated with the role of ionic liquid in enhancing the transportation of photo-induced electrons and hole in the photocatalyst nanocomposite. As an excellent result, higher photocatalytic efficiency is obtained by the S2 sample with 0.010 w% of TiO_2 with a thickness of 40 µm. According to the antibacterial results obtained based on Kirby-Bauer method and membrane permeability assessments, it is clear that a higher visible light photocatalytic degradation activity support a higher antibacterial activity due to the positive correlation between

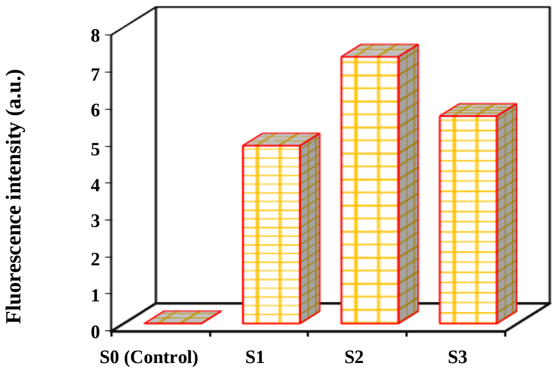

Fig. 9: Oxidative stress investigation based on ROS generation against the clinical strain of Bacillus under visible light irradiation over different samples.

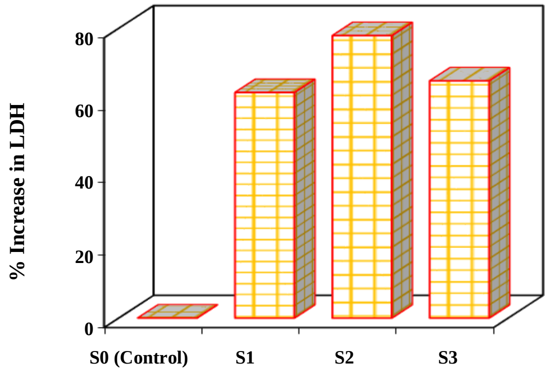

Fig. 10: Cell permeability as exemplified by LDH quantification against the clinical strain of Bacillus under visible light irradiation over the different samples.

the photocatalytic activity and antibacterial activity of the nanocomposite films. It is worthy to note, by virtue of its application, the prepared this new type of nanocomposite could be a good nanotechnological product which has a gigantic potential in the commercialization for possible industrial and medical applications.

Nomenclature

PMMA/IL-TiO_2	Poly(methyl methacrylate)/ Ionic liquid-TiO_2
IL	Ionic liquid
[bmim][BF_4]	1-buthyl-3-methylimidazolium tetrafluoroborate
BET	Bruner-Emmet-Teller
MMA	Methyl methacrylate
TX-100	Triton X-100
S_n	Sample number
DRS	Diffuse Reflectance Spectra
TEM	Transmission Electron Microscopy
TGA	Thermal Gravimetric Analysis
C_o	Initial concentration of TB at zero time
C_t	Concentration of TB at *t* time
k	Rate constant
ROS	Reactive Oxygen Species
pHPZC	pH point of zero charge (pHPZC)
LDH	Lactate dehydrogenase

Acknowledgments

The financial support from ARAK University Research Council is gratefully acknowledged (grant no. 93/5251)

Received : Apr. 17, 2018 ; Accepted : Jun. 18, 2018

REFERENCES

[1] Singh S., Mahalingam H., Kumar Sing P., Polymer-Supported Titanium Dioxide Photocatalysts for Environmental Remediation: A Review, *Appl. Catal. A General*, **462-463**: 178-195 (2013).

[2] Mirhoseini F., Salabat A., Ionic Liquid Based Microemulsion Method for Fabrication of Poly(methyl methacrylate)–TiO_2 Nanocomposite as Highly Efficient Visible Light Photocatalyst, *RSC Adv.*, **5**: 12536-12545 (2015).

[3] Yang M., Di Z., Lee J.K., Facile Control of Surface Wettability in TiO_2/poly(methyl methacrylate) Composite Films, *J. Colloid Interf. Sci.*, **368**: 603-607 (2012).

[4] Ratova M., Mills V., Antibacterial Titania-Based Photocatalytic Extruded Plastic Films, *J. Photoch. Photobio. A Chemistry*, **299**: 159-165 (2015).

[5] Sannino D, Vaiano V, Sacco O., Ciambelli P., Mathematical Modelling of Photocatalytic Degradation of Methylene Blue under Visible Light Irradiation, *J. Environ. Chem. Eng.*, **1**: 56-60 (2013).

[6] Patchaiyappan A, Saran S., Devipriya S.P., Recovery and Reuse of TiO2 Photocatalyst from Aqueous Suspension Using Plant Based Coagulant - A Green Approach, *Korean J. Chem. Eng.*, **33**: 2107-2113 (2016).

[7] Sriwong C., Wongnawa S., Patarapaiboolchai O., Photocatalytic Activity of Rubber Sheet Impregnated with TiO_2 Particles and Its Recyclability, *Catal. Commun.*, **9**: 213-218 (2008).

[8] Rizzoa L., Kochb J., Belgiornoa V., Andersonb M., Removal of Methylene Blue in a Photocatalytic Reactor Using Polymethylmethacrylate Supported TiO_2 Nanofilm, *Desalination*, **211**: 1-9 (2007).

[9] Pelaez M., Nolan N.T., Pillai S.C., Seery M.K., Falaras P., Kontos A.G., Dunlop P.S.M., Hamilton J.W.J., Byrne J.A., O'Shea K., Entezari M.H., Dionysiou D.D., A Review on the Visible Light Active Titanium Dioxide Photocatalysts for Environmental Applications, *Appl. Catal. B Environmental*, **125**: 331-349 (2012).

[10] Wang X., Zhang K., Guo X., Shen G., Xiang J., Synthesis and Characterization of N-Doped TiO2 Loaded onto Activated Carbon Fiber with Enhanced Visible-Light Photocatalytic Activity, *New J. Chem.*, **38**: 6139-6146 (2014).

[11] Janitabar Darzi S., Movahedi M., Visible Light Photodegradation of Phenol Using Nanoscale TiO2 and ZnO Impregnated with Merbromin Dye: A Mechanistic Investigation, *Iran. J. Chem. Chem. Eng. (IJCCE)*, **33**: 55-64 (2014).

[12] Kamegawa T., Imai H., Yamashita H., Design of Visible Light Sensitive Heterogeneous Photocatalyst by Utilization of Sulfocalixarene as a Linker of Zinc Porphyrin and Pt-TiO2, *Bull. Chem. Soc. Jpn.*, **89**: 743-745 (2016).

[13] Ravishankar T.N., Ramakrishnappa T., Nagabhushana H., Souza V.S., Dupont J., Nagaraju G., Hydrogen Generation and Degradation of Trypan Blue Using Fern-Like Structured Silver-Doped TiO_2 Nanoparticles, *New J. Chem.*, **39**: 1421-1429 (2015).

[14] Fernandez C., Larrechi M.S., Callao M.P., An Analytical Review of Processes for Removing Organic Dyes from Wastewater Effluents, *Trends Anal. Chem.*, **29**: 1202-1211 (2010).

[15] State of California Environmental Protection Agency Office of Environmental Health Hazard Assessment Safe Drinking Water and Toxic Enforcement act of 1986- Chemicals Known to the State to Cause Cancer or Reproductive Toxicity, September 11, (2009).

[16] Kasanen J., Salstela J., Suvanto M., Pakkanen T.T., Photocatalytic Degradation of Methylene Blue Dye Using Fe_2O_3/TiO_2 Nanoparticles Prepared by Sol-Gel Method, *Appl. Surf. Sci.*, **258**: 1738–1743 (2011).

[17] Akpan U.G., Hameed B.H., Parameter Affecting the Photocatalytic Degradation of Dye Using TiO_2-Based Photocatalysts: A Review, *J. Hazard. Mater.*, **170**: 520-529 (2009).

[18] Elfeky S.A., Al-Sherbini A.A., Photocatalytic Decomposition of Trypan Blue over Nanocomposite Thin Films, *Kinet. Catal.*, **52**: 391-396 (2011).

[19] Mirhoseini F., Salabat A., Removal of Methyl Tert-Butyl Ether as a Water pollutant by Photodegradation over a New Type of Poly(methyl methacrylate)/TiO_2, *Polym. Composites*, **39**: 1248-1254 (2016).

[20] Salabat A., Mirhoseini F., A Novel and Simple Microemulsion Mthod for Synthesis of Biocompatible Functionalized Gold Nanoparticles, *J. Mol. Liq.* **268**: 849–853 (2018).

[21] Salabat A., Mirhoseini F., Valirasti R., Engineering poly(methyl methacrylate)/Fe_2O_3 Hollow Nanospheres Composite Prepared in Microemulsion System as a Recyclable Adsorbent for Removal of Benzothiophene, *Ind. Eng. Chem. Res*. **58**: 17850-17858 (2019).

[22] Salabat A., Mirhoseini F., Photo-Induced Hydrophilicity Study of Poly(methyl methacrylate)/TiO_2 Nanocomposite Prepared in Ionic Liquid Based Microemulsion System, *Curr. Appl. Polym. Sci.*, 2018, *2*, 112-120.

[23] Salabata A., Mirhoseini F., Abdoli K., A Microemulsion Route to Fabrication of Mono- and bi-Metallic Cu/Zn/-Al_2O_3 Nanocatalysts for Hydrogenation Reaction, *Scientia Iranica* C **25**(3): 1364-1370 (2018).

[24] Mirhoseini F., Salabat A., Photocatalitic Filter. US Patent 20180104678 A1 (Appl No. 15/839851), 2018.

[25] Yu J.G., Xiang Q.J., Zhou M.H., Preparation, Characterization and Visible-Light-Driven Photocatalytic Activity of Fe-Doped Titania Nanorods and First-Principles Study for Electronic Structures, *Appl. Catal. B Environmental*, **90**: 595-602 (2009).

[26] Mohammadi R, Massoumi B., Rabani M., Photocatalytic Decomposition of Amoxicillin Trihydrate Antibiotic in aqueous Solutions under UV Irradiation Using Sn/TiO_2 Nanoparticles, *Int. J. Photoenergy*, **2012**: 1-11(2011).

[27] Tamboli M.S., Kulkarni M.V., Rajendra H., Patil R.H., Gade W.N., Shalaka C., Navale S.N., Kale B.B., Nanowires of Silver–Polyaniline Nanocomposite Synthesized via in Situ Polymerization and Its Novel Functionality as an Antibacterial Agent, *Colloid Surf. B Biointerfaces*, **92**: 35-41 (2012).

[28] Habibi G., Arjomandzadegan M., Tayeboon M., Didgar F., Sarmadian H., Sadrnia M., Mirhosseini F., Geravand S., Abdoli M., Comparison of Antibacterial Effects of a Carrier Produced in Microemulsion System from Aqueous Extract of Aloe Vera with Selected Antibiotics on Enterobacteriacea, *Iran. J. Microbiol.*, **10**: 334-341 (2018).

[29] Gilani S., Ghorbanpour M., Parchehbaf Jadid A., Antibacterial Activity of ZnO Films Prepared by Anodizing, *J. Nanostruct. Chem.*, **6**: 183–189 (2016).

[30] Salabat A., Mirhoseini F., Applications of a New Type of Poly(methyl methacrylate)/TiO_2 Nanocomposite as an Antibacterial Agent and Reducing Photocatalyst, *Photochem. Photobiol, Sci.*, **5**: 1637-1643 (2015).

[31] Brunet L., Lyon D.Y., Hotze E.M., Alvarez P.J.J., Wiesner M.R., Comparative Photoactivity and Antibacterial Properties of C60 Fullerenes and Titanium Dioxide Nanoparticles, *Environ. Sci. Technol*., **43**: 4355-4360 (2009).

[32] Wang H., Joseph J.A., Quantifying Cellular Oxidative Stress by Dichlorofluorescein Assay Using Microplate Reader, *Free Radical Biol. Med*., **27**: 612-616 (1999).

[33] Stylidi M., Kondarides D.I., Verykios X.E., Pathways of Solar Lightinduced Photocatalytic Degradation of Azo Dyes in Aqueous TiO_2 Suspensions, *Appl. Catal. B Environmental*, **40**: 271–286 (2003).

[34] Bandara J., Mielczarski J. A., Kiwi J., Photosentized Degradation of Azo Dyes on Fe, Ti, and All Oxides. Mechanisem of Charge Transfer During the Degradation, *Langmuir*, **15**: 7680-7687 (1999).

[35] Sangchakr B., Hisanaga T., Tanaka K., Photocatalytic Degradation of Sulfonated Aromatics in TiO_2 Suspension, *J. Photochem Photobiol. A Chemistry*, **85**: 187-190 (1995).

[36] Galindo C., Jacques P., Kalt A., Photodegradation of the Aminoazobenzene Acid Orange 52 by three Advanced Oxidation Processes: UV/H_2O_2, UV/TiO_2 and VIS/TiO_2 Comparative Mechanistic and Kinetic Investigations, *J. Photochem. Photobiol. A Chemistry*, **130**: 35-47 (2000).

[37] Daneshvar N., Salari D., Khataee, A.R., Photocatalytic Degradation of Azo Dye Acid Red 14 in Water: Investigation of the Effect of Operational Parameters, *J. Photochem. Photobiol. A Chemistry*, **157**: 111–116 (2003).

[38] Seddigi Z.S., Ahmed S.A., Bumajdad A., Danish E.Y., Shwaky A.M., Gondal V., Soylak M., The Efficient Photocatalytic Degradation of Methyl Tert-Butyl Ether under Pd/Zno and Visible Light Irradiation, *Photochem. Photobiol.*, **91**: 265-271 (2015).

[39] Reutergårdh L.B., Iangphasuk M., Photocatalytic Decolourization of Reactive Azo Dye: a Comparison Between TiO_2 and CdS Photocatalysis, *Chemosphere*, **35**: 585-596 (1997).

[40] Poulios I., Tsachpinis I., Photodegradation of the Textile Dye Reactive Black 5 in the Presence of Semiconducting Oxides, *J. Chem. Technol. Biotechnol.*, **74**: 349-357 (1995).

[41] Hernández-Gordillo A., Romero A.G., Tzompantzi F., Oros-Ruiz S., Gómez R., Visible Light Photocatalytic Reduction of 4-Nitrophenol Using cds in the Presence of Na_2SO_3, *J. Photoch. Photobio. A Chemistry*, **257**: 44-49 (2013).

[42] Matsunaga T., Tomoda R., Nakajima T., Wake H., Photoelectrochemical Sterilization of Microbial Cells by Semiconductor Powders, *FEMS Microbiol. Lett.*, **29:** 211–214 (1985).

[43] Robertson P.K.J., Robertson J.M.C., Bahnemann D.W., Removal of Microorganisms on Their Chemical Metabolites from Water Using Semiconductor Photocatalysis, *J. Hazard. Mater.*, **211-212**: 161-171 (2012).

[44] Dunlop P.S.M., Sheeran C.P., Byrne J.A., McMahon M.A.S., Boyle M.A., McGuigan K. G., Inactivation of Clinically Relevant Pathogens by Photocatalytic Coatings, *J. Photoch. Photobio. A Chemistry*, **216**, 303-310 (2012).

[45] Foster H., Ditta I., Varghese S., Steele V., Photocatalytic Disinfection Using Titanium Dioxide: Spectrum and Mechanism of Antimicrobial Activity, *Appl. Microbiol. Biotechnol*., **90**: 1847-1868 (2011).

[46] Nadtochenko V., Denisov N., Sarkisov O., Gumy D., Pulgarin C., Kiwi J., Laser Kinetic Spectroscopy of the Interfacial Charge Transfer between Membrane Cell Walls of E. Coli and TiO_2, *J. Photochem. Photobiol. A Chemistry*, **181**: 401-407 (2006).

[47] Hebeish A.A., Abdehady M.M., Youssef A.M., TiO_2 Nanowire and TiO_2 Nanowire Doped Ag-PVP Nanocomposite for Antimicrobial and Self-Cleaning Cotton Textile, *Carbohyd. Polym.*, **91**: 549-559 (2013).

[48] Pablos C., J. Marugán J., vanGrieken R., Serrano E., Emerging Micropollutant Oxidation During Disinfection Processes using UV-C, UV-C/H_2O_2, UV-A/TiO_2 and UV-A/TiO_2/H_2O_2, *Water Res.*, **47**: 1237–1245 (2013).

[49] Liu X., Hong H., Wu X., Wu Y., Ma Y., Guan W., Ye Y., Synthesis of TiO_2–Reduced Graphene Oxide Nanocomposites for Efficient Adsorption and Photodegradation of Herbicides, *Water, Air, & Soil Pollution*, **227**: 21-30 (2016).

[50] Salabat A., Mirhoseini F., Mahdieh M., Saydi H., A Novel Nanotube-Shaped Polypyrrole–Pd Composite Prepared Using Reverse Microemulsion Polymerization and Its Evaluation as an Antibacterial Agent, *New J. Chem.*, **39**: 4109-4114 (2015).

[51] Boomi P., Prabu H.G., Mathiyarasu J., Synthesis, Characterization and Antibacterial Activity of Polyaniline/Pt-Pd Nanocomposite, *Eur. J. Med. Chem.*, **72**: 18-25 (2014).

[52] Salabat A., Farid Mirhoseini F., Mohammad Arjomandzadegan M., Jiryaei E., A Novel Methodology for Fabrication of Ag–Polypyrrole Core–Shell Nanosphere Using Microemulsion System and Evaluation of Its Antibacterial Application, *New J. Chem*., **41**: 12892-12900 (2017).

[53] Mirhoseinia F., Alireza Salabata A., Antibacterial Activity Based poly(methyl methacrylate) Supported TiO_2 Photocatalyst Film Nanocomposite, *Tech. J. Engin. App. Sci*., **5** (1): 115-118 (2015).

[54] Alireza Salabata A., Mirhoseinia F., Masoumia Z., Mahdie M., Preparation and Characterization of Polystyrene-Silver Nanocomposite Using Microemulsionmethod and Its Antibacterial Activity, *JNS*, **4**: 377-382 (2014).

Supplementary Materials

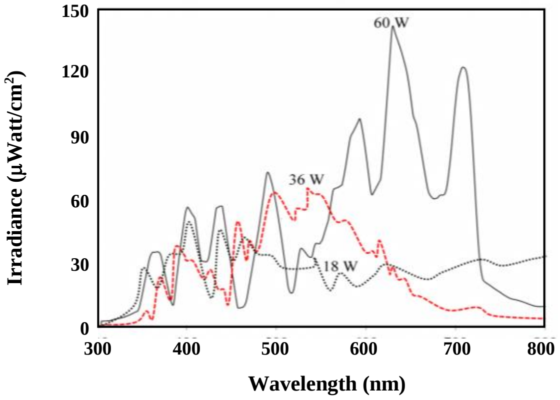

Fig. ES1: Emission spectrum of the various light source used in photocatalytic reduction.

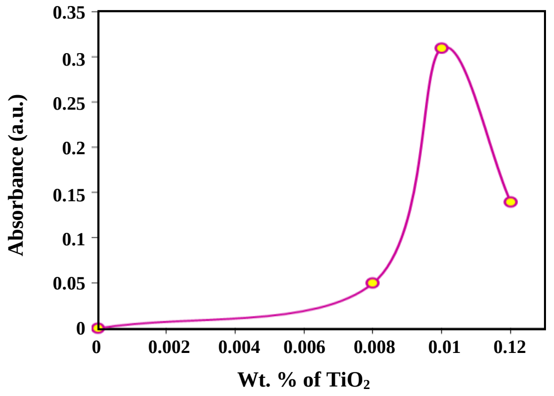

Fig. ES2: Hydroxyl radical amounts obtained using modified PMMA/IL-TiO_2 nanocomposite at different TiO_2 content under visible light irradiation for 60 min.

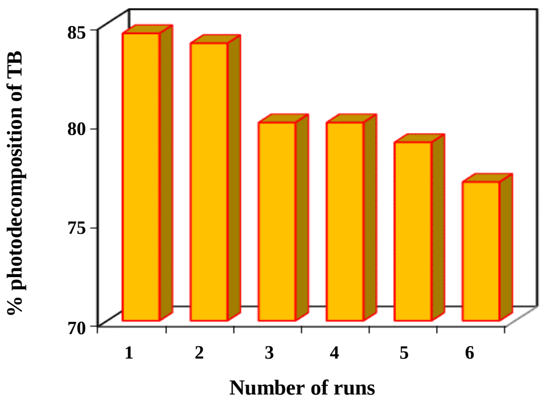

Fig. ES3: Effect of initial dye concentration on the photocatalytic degradation of TB dye over S2 sample under visible light irradiation.